Supplementary Material

Novel Chiral-Driven Stereoisomerism Dimension of Fire Safety and Crystallization Mechanisms in Poly(lactic acid)

Xue-Min Yang [a], Jin-Xiang Lv [b], Kathrin Harre [a], and Dan Xiao [a]*

[a] Fakultät Landbau/Umwelt/Chemie, Hochschule für Technik und Wirtschaft Dresden, Friedrich-List-Platz 1, D-01069 Dresden, Germany

[b] Department of Materials Science and Engineering, Fujian University of Technology, Fuzhou, Fujian, 350108, China

Corresponding author:
*Email: xiaodan2014@gmail.com,

Methods

Materials

The (S)-(+)-1,1'-binaphthyl-2,2'-diyl hydrogen phosphate (L (+)), and (R)-(-)-1,1'-binaphthyl-2,2'-diyl hydrogen phosphate (R (-)) were obtained from Aladdin company (China). PLLA (3052D, a density of 1.24g/cm3) was purchased from Nature Work. PDLA (D120) (stereochemical purity ≥ 99%, a density of 1.24g/cm3, flow index of 25g/10min at 210 °C) were purchased from Total Corbin Co., Ltd. (Thailand). PMLA was the mixture of PLLA (L130) and PDLA (D120) (mass ratio was 1 :1) in our laboratory.

Fabrication of right (R (-)) and left (L (+) chiral flame retardants for bio-based polylactide (PLA)

First of all, the raw materials (PLLA (L130), PDLA (D120), (R)-(-)-1,1'-binaphthyl-2,2'-diyl hydrogen phosphate (R (-)) and (S)-(+)-1,1'-binaphthyl-2,2'-diyl hydrogen phosphate (L (+)) were dried firstly. According to the formula in Table 1S (Supporting Information), the functional PLA composites were processed at a speed of 70rpm at 175 °C for 7 minutes. Then, the different sizes of functional PLA composites were formed using a CREE-6014A-30 Heat Press for the standard testing at 190 °C.

Characterizations

TGA testing was investigated by a TGA/DSC 200F3 Netzsch over the temperature range of 40–700 °C under N_2 at 10 K·min^{-1}. SEM combined with EDS was examined by NovaNano 450 T and JEOL JSM-6700F measurement. The UL-94 vertical burning (13 mm × 130 mm × 3 mm) measurement was conducted on a CZF-2 Jiangning instrument in accordance with ASTM D 3801 standard. LOI (6.5 mm × 120 mm × 3 mm) measurement was investigated by a JF-3 Jiangning instrument in accordance with ASTM D2863 standard. Cone-calorimeter (100 mm × 3 mm × 100 mm) measurement was investigated by a FTT instrument (35 kW/m^2, Britain) in accordance with ISO 5660-1 standard. Differential scanning calorimetry (DSC) measurement was investigated by a Netzsch instrument. First of all, the temperature for non-isothermal testing was raised from 35 to 200 ˚C under N_2 at 10 K·min^{-1}. Then the temperature for non-isothermal testing dropped from 200 to 35˚C. Afterwards, the temperature for non-isothermal testing was raised to 200 ˚C. The crystalline degree (Xc) was obtained from the following equation:

$$Xc = \frac{\Delta Hm}{(1-\varphi)\ \Delta H_m^o} \times 100\%$$

For isothermal crystallization testing, the specimen (5-10 mg) was firstly treated with the same procedure at 80 K·min^{-1} to eliminate thermal history on a DSC 200F3 Netzsch under N_2, and then cooled to a predetermined temperature (100°C, 105°C, 110°C, 115°C) and record the curve of isothermal crystallization. Polarizing optical microscope (POM) was conducted on a DM 2700P LEICA instrument. X-ray powder diffractometer (XRD) measurement was conducted on a D8ADVANCE instrument. Carbon residues were recorded by a Dajiang digital camera instrument. SEM testing of carbon residues was recorded by a JEOL JSM-6700F measurement. XPS and Raman measurements were conducted on a PHI5300 spectrometer and Fisher DxRxi instruments. TG-FTIR measurement was recorded by the TG209F1 measurement at 10 $K·min^{-1}$ under 40–750 ˚C combined with Vertex70 instrument from 4000 to 400 cm^{-1} measurements under N_2. Py-GCMS measurement was recorded by using an Agilent 5977 B combined with 8790 B instruments under N_2.

1. Fig. Captions

Fig. S1. The SPR curves of PLA/5% R (-) and PLA/5% L (+) compounds

Fig. S2. The COP curves of PLA/5% R(-) and PLA/5% L(+) compounds

Fig. S3. The weight loss curves of PLA/5%R(-) and PLA/5%L(+) compounds

Fig. S4. Crystallization curves of PDLA with R(-)/L(+) compounds (a), PLLA with **R(-)/L(+)** compounds (b) and PMLA with R(-)/L(+) compounds (c)

Fig. S5. The crystallinityof PLA with R(-) or PLA/L(+) compounds. Melting behaviors of PDLA with R(-)/L(+) compounds (a), PLLA with R(-)/L(+) compounds (b) and PMLA with R(-)/L(+) compounds (c). The isothermal crystallinity of PLA with R(-) or PLA/L(+) compounds at different temperatures (d1-e4). The curves $\ln(-\ln(1-X(t)))$ and $\ln(t)$ of of PLA with R(-) or PLA/L(+) compounds at different temperatures (f1-g4)

Fig. S6. TGA (a) and DTG (b) curves of PDLA with R(-)/L(+), PLLA with R(-)/L(+)nd PMLA with R(-)/L(+) compounds

Fig. S7. The morphology of the R (-) or L (+) flame retardants in PLA. The SEM images of PDLA (a), PDLA/5%R(-) (d), PDLA/5%L(+) (g), PLLA (b), PLLA/5%R(-) (e), PDLA/5%L(+) (h), PMLA (c), PMLA/5%R(-) (f), PLMA/5%L(+) (i) compounds

Fig. S8. The energy spectrum of the R (-) or L (+) flame retardants in PLA. The EDS images of PDLA (a), PDLA/5%R(-) (d), PDLA/5%L(+) (g), PLLA (b), PLLA/5%R(-) (e), PDLA/5%L(+) (h), PMLA (c), PMLA/5%R(-) (f), PLMA/5%L(+) (i) compounds

Fig. S9. The digital images of carbon residues after cone calorimetry tests. The vertical (a1) and side view (a2) images of PDLA/5%R(-) compound; the vertical (b1) and side view (b2) images of PDLA/5%L(+) compound; the vertical (c1) and side view (c2) images of PLLA/5%R(-) compound; the vertical (d1) and side view (d2) images of PLLA/5%L(+) compound; the vertical (e1) and side view (e2) images of PMLA/5%R(-) compound; ; the vertical (f1) and side view (f2) images of PMLA/5%L(+) compound

Fig. S10. The SEM images of carbon residues after cone calorimetry test. The SEM images of PDLA/5%R(-) (a), PDLA/5%L(+) (d), PLLA/5%R(-) (b), PLLA/5%L(+) (e), PMLA/5%R(-) (c), and PMLA/5%L(+) (f) compounds

Fig. S11. The EDS results of carbon residues after cone calorimetry test. The EDS, phosphorus spectrum, and element contents of PDLA/5%R(-) (a1-a3), PDLA/5%L(+) (b1-b3), PLLA/5%R(-) (c1-c3), PLLA/5%L(+) (d1-d3), PMLA/5%R(-) (e1-e3), and PMLA/5%L(+) (f1-f3) compounds

Fig. S12. The Raman spectra of carbon residues after cone calorimetry test. The Raman results of PDLA/5%R(-) (a), PDLA/5%L(+) (b), PLLA/5%R(-) (c), PLLA/5%L(+) (d), PMLA/5%R(-) (e), and PMLA/5%L(+) (f) compounds

Fig. S13. The XPS results of carbon residues after cone calorimetry test. The XPS, C1s, O1s and P2p of PDLA/5%R(-) (a1-a4), PDLA/5%L(+) (b1-b4), PLLA/5%R(-) (c1-c4), PLLA/5%L(+) (d1-d4), PMLA/5%R(-) (e1-e4), and PMLA/5%L(+) (f1-f4) compound

Fig. S14. Pyrolysis behavior in vapor phase. Three dimensions degradation of PDLA/5%R(-) (a1), PDLA/5%L(+) (a2), PLLA/5%R(-) (b1), PLLA/5%L(+) (b2), PMLA/5%R(-) (c1), and PMLA/5%L(+) (c2) compounds. TG-FTIR curves of PLA PDLA/5%R(-) (d1), PDLA/5%L(+) (d2), PLLA/5%R(-) (e1), PLLA/5%L(+) (e2), PMLA/5%R(-) (f1), and PMLA/5%L(+) (f2) compounds at different temperatures; the hydrocarbons (g), aldehydes (h), and carbonyl compounds (1) at different temperatures

Fig. S15. The Py-GSMS results of (R)-(-)-1,1'-binaphthyl-2,2'-diyl hydrogen phosphate (R (-) flame retardant), and (S)-(+)-1,1'-binaphthyl-2,2'-diyl hydrogen phosphate (L (+) flame retardant), the keep time of R (-) and L (+) flame retardants (a), the main mass spectrometry of R (-) and L (+) flame retardants (b-e)

2. Table captions

Table S1. Formula of functional PLA composites

Table S2. The results of functional PLA composites in UL-94 and LOI tests

Table S3. The cone calorimeter results of functional PLA composites

Table S4. The non-isothermal crystallization results of functional PLA composites

Table S5. The isothermal crystallization results of functional PDLA composites

Table S6. The isothermal crystallization results of functional PLLA composites

Table S7. Related thermal stability data for functional PLA composites under N_2

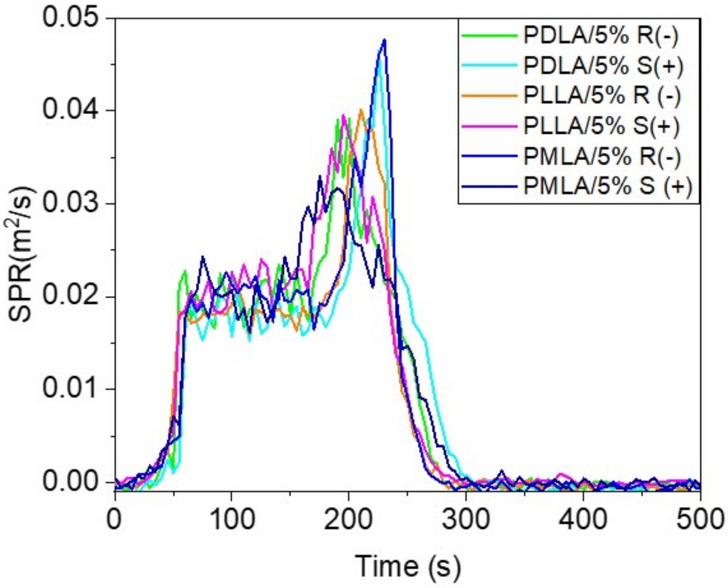

Fig. S1. The SPR curves of PLA/5% R (-) and PLA/5% L (+) compounds

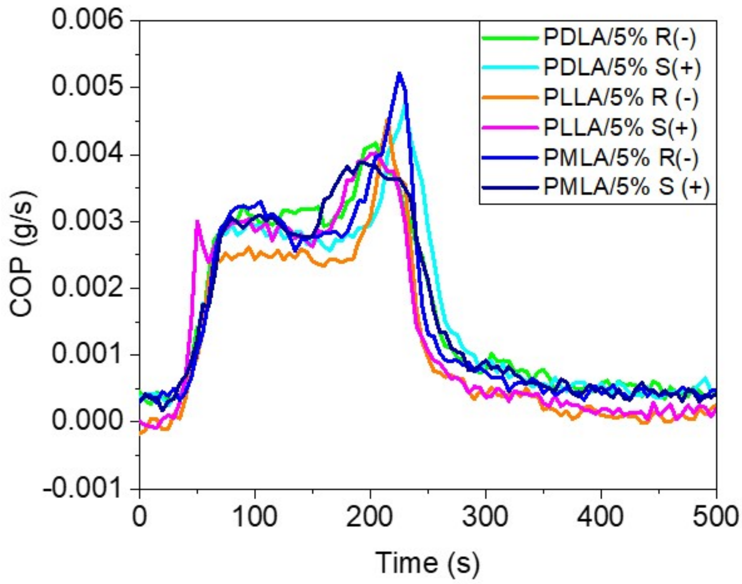

Fig. S2. The COP curves of PLA/5% R(-) and PLA/5% L(+) compounds

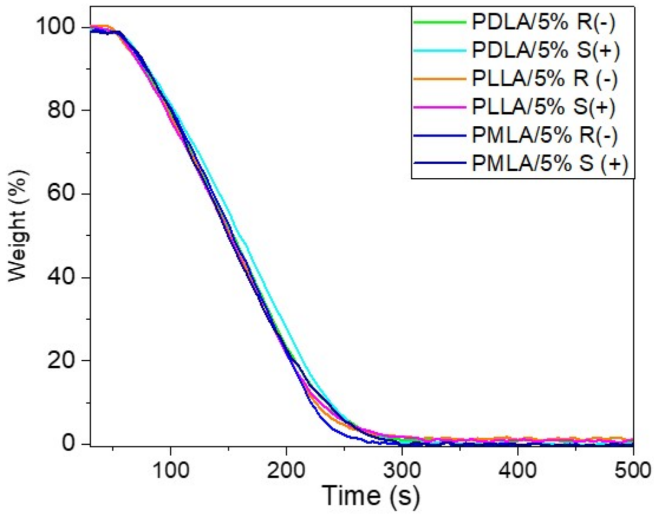

Fig. S3. The weight loss curves of PLA/5%R(-) and PLA/5%L(+) compounds

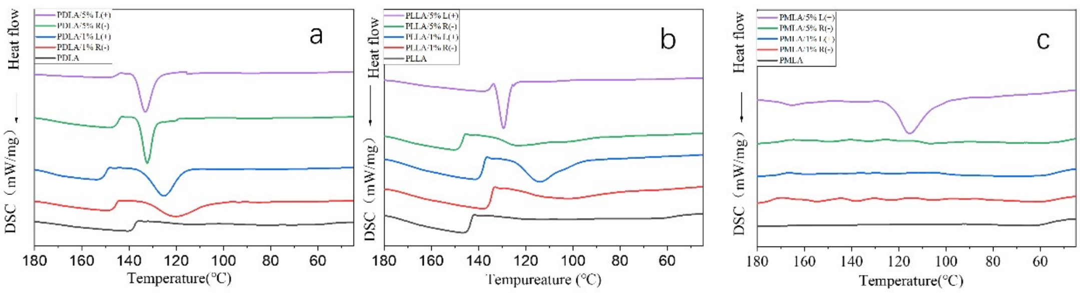

Fig. S4. Crystallization curves of PDLA with R(-)/L(+) compounds (a), PLLA with R(-)/L(+) compounds (b) and PMLA with R(-)/L(+) compounds (c)

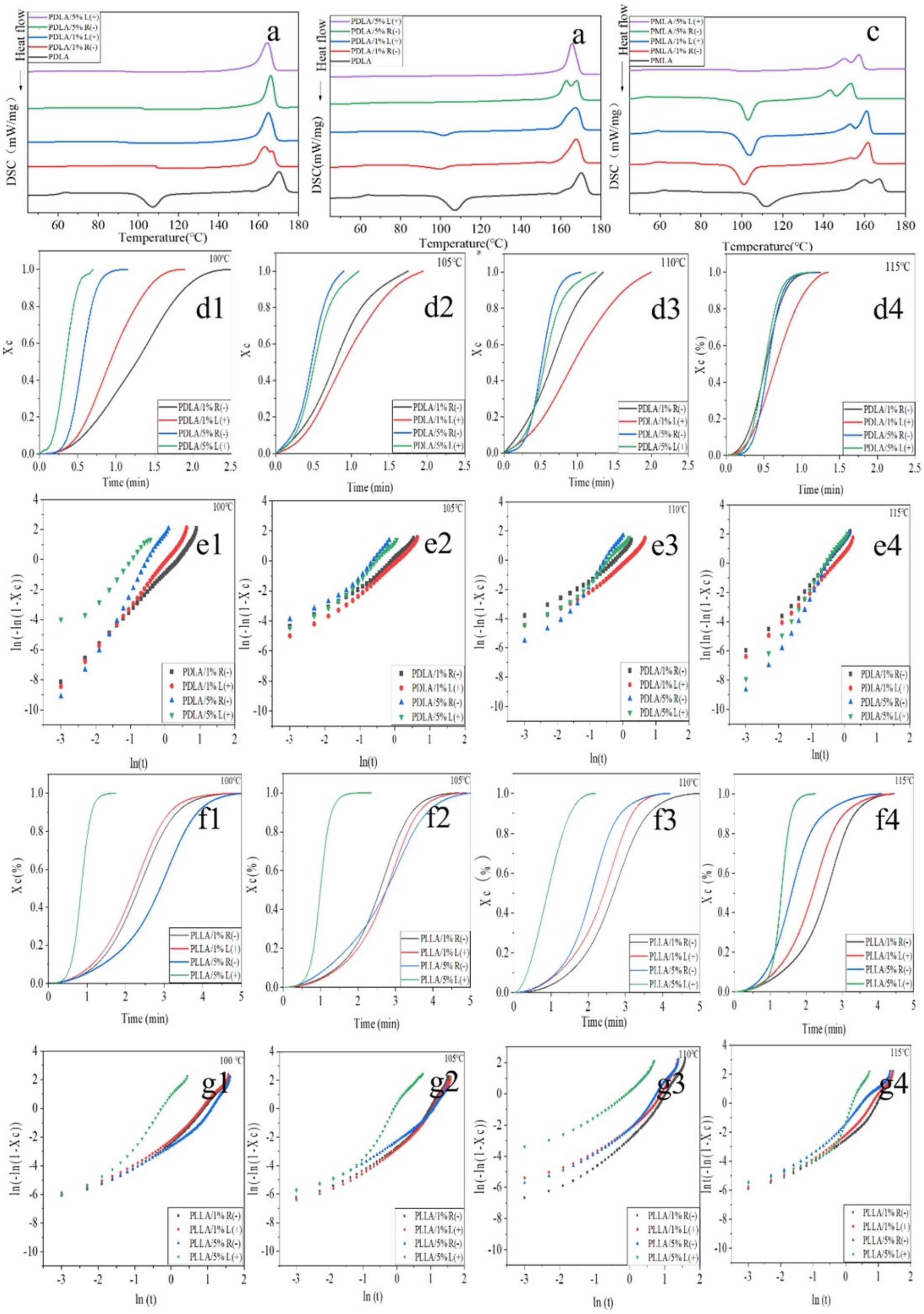

Fig. S5. The crystallinityof PLA with R(-) or PLA/L(+) compounds. Melting behaviors of PDLA with R(-)/L(+) compounds (a), PLLA with R(-)/L(+) compounds (b) and PMLA with R(-)/L(+) compounds (c). The isothermal crystallinity of PLA with R(-) or PLA/L(+) compounds at different temperatures (d1-e4). The curves ln(−ln(1−X(t))) and ln(t) of of PLA with R(-) or PLA/L(+) compounds at different temperatures (f1-g4)

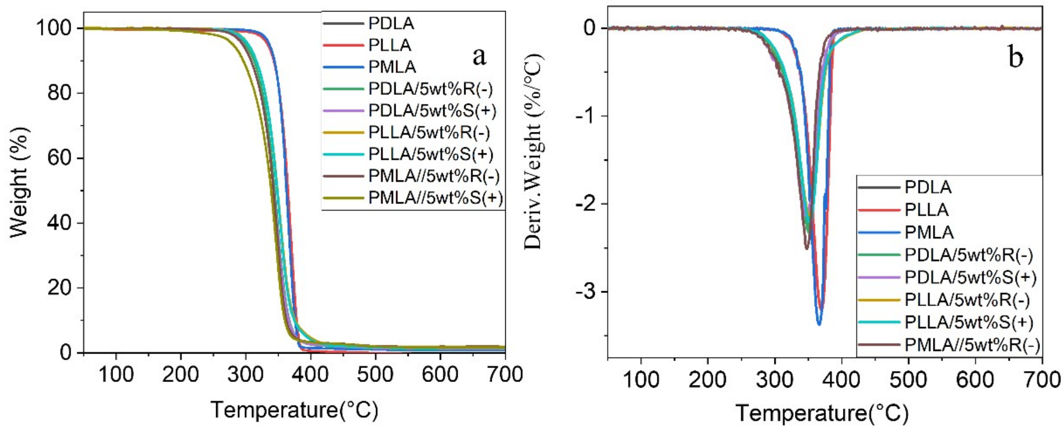

Fig. S6. TGA (a) and DTG (b) curves of PDLA with R(-)/L(+), PLLA with R(-)/L(+)nd PMLA with R(-)/L(+) compounds

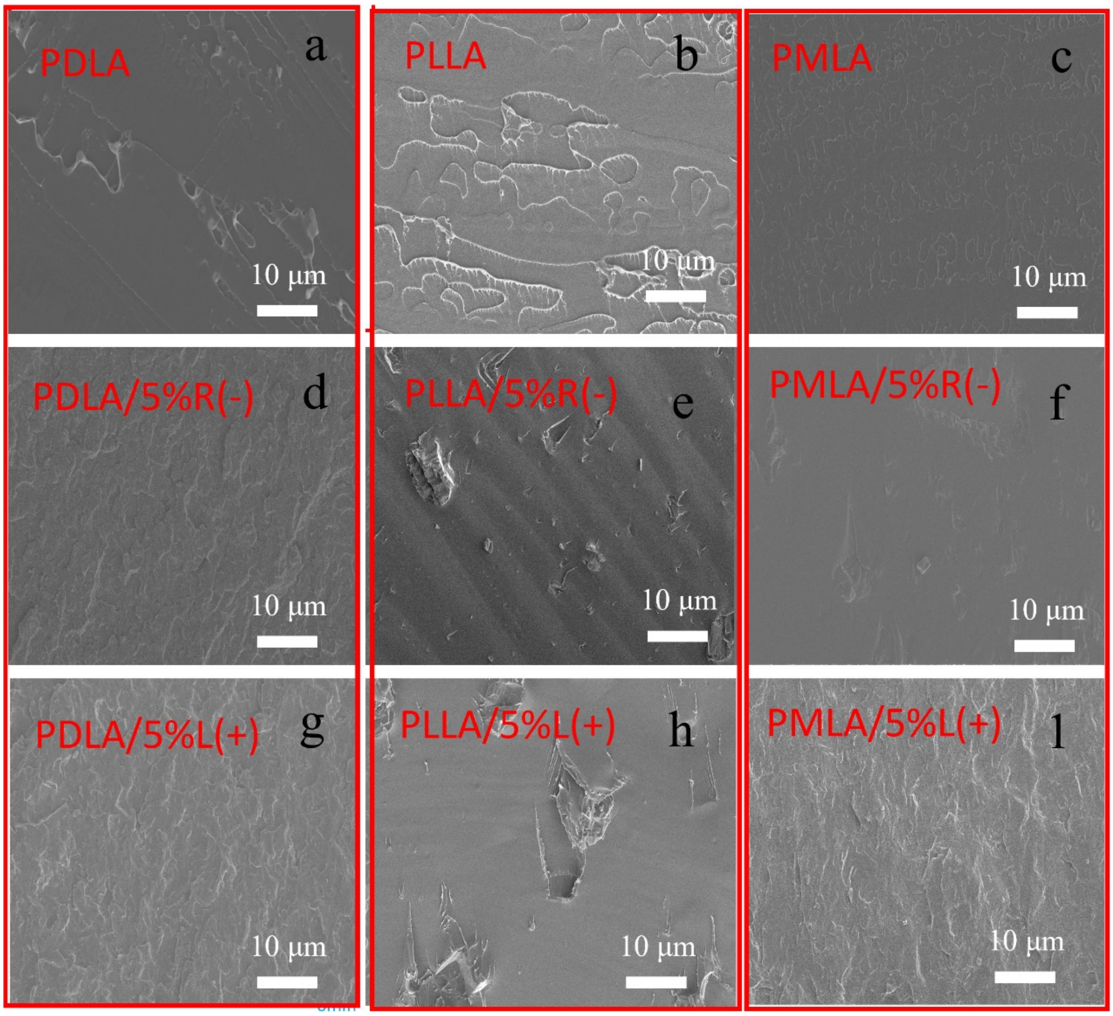

Fig. S7. The morphology of the R (-) or L (+) flame retardants in PLA. The SEM images of PDLA (a), PDLA/5%R(-) (d), PDLA/5%L(+) (g), PLLA (b), PLLA/5%R(-) (e), PDLA/5%L(+) (h), PMLA (c), PMLA/5%R(-) (f), PLMA/5%L(+) (i) compounds

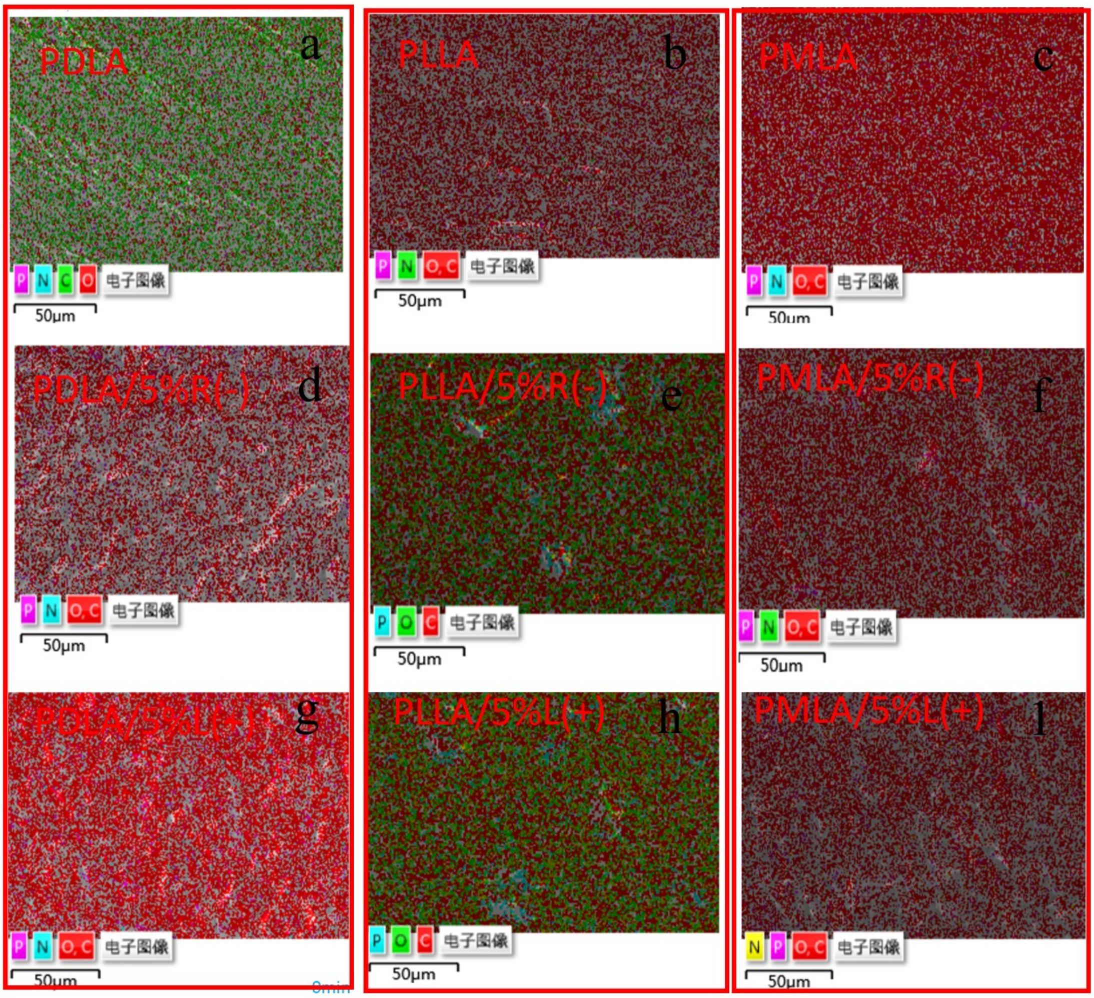

Fig. S8. The energy spectrum of the R (-) or L (+) flame retardants in PLA. The EDS images of PDLA (a), PDLA/5%R(-) (d), PDLA/5%L(+) (g), PLLA (b), PLLA/5%R(-) (e), PDLA/5%L(+) (h), PMLA (c), PMLA/5%R(-) (f), PLMA/5%L(+) (i) compounds

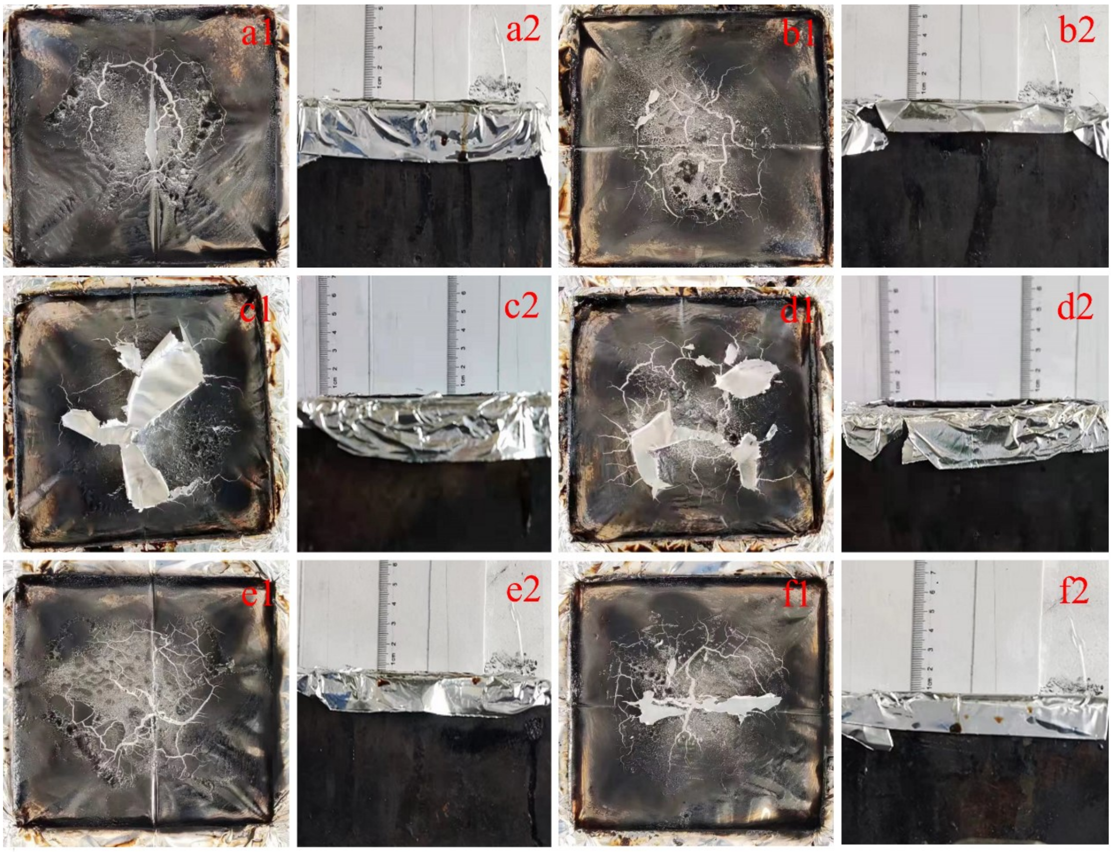

Fig. S9. The digital images of carbon residues after cone calorimetry tests. The vertical (a1) and side view (a2) images of PDLA/5%R(-) compound; the vertical (b1) and side view (b2) images of PDLA/5%L(+) compound; the vertical (c1) and side view (c2) images of PLLA/5%R(-) compound; the vertical (d1) and side view (d2) images of PLLA/5%L(+) compound; the vertical (e1) and side view (e2) images of PMLA/5%R(-) compound; ; the vertical (f1) and side view (f2) images of PMLA/5%L(+) compound

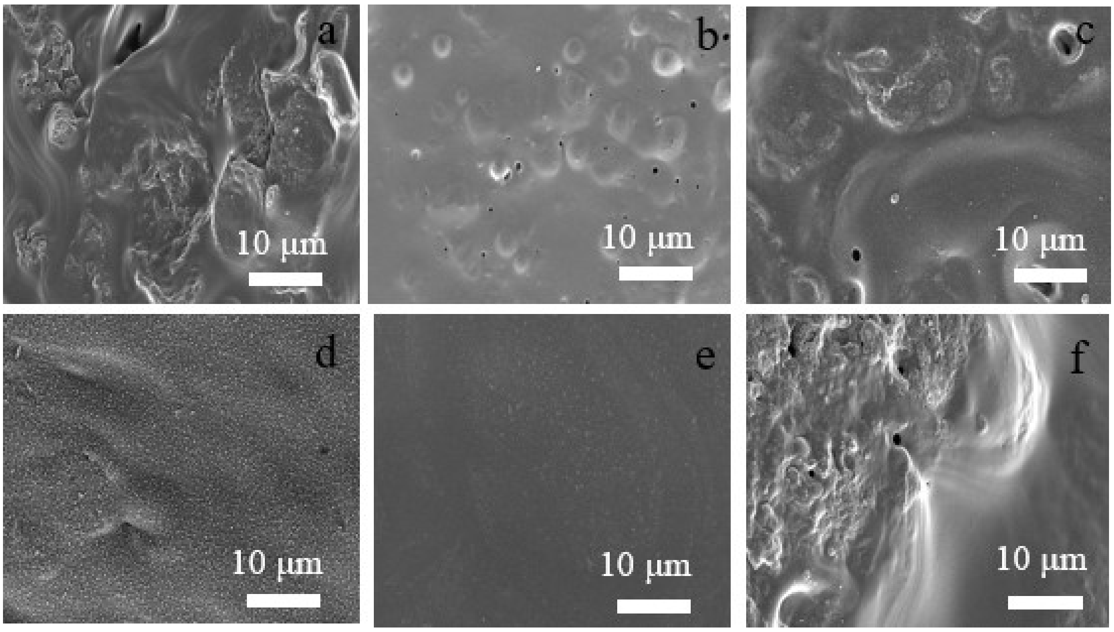

Fig. S10. The SEM images of carbon residues after cone calorimetry test. The SEM images of PDLA/5%R(-) (a), PDLA/5%L(+) (d), PLLA/5%R(-) (b), PLLA/5%L(+) (e), PMLA/5%R(-) (c), and PMLA/5%L(+) (f) compounds

.

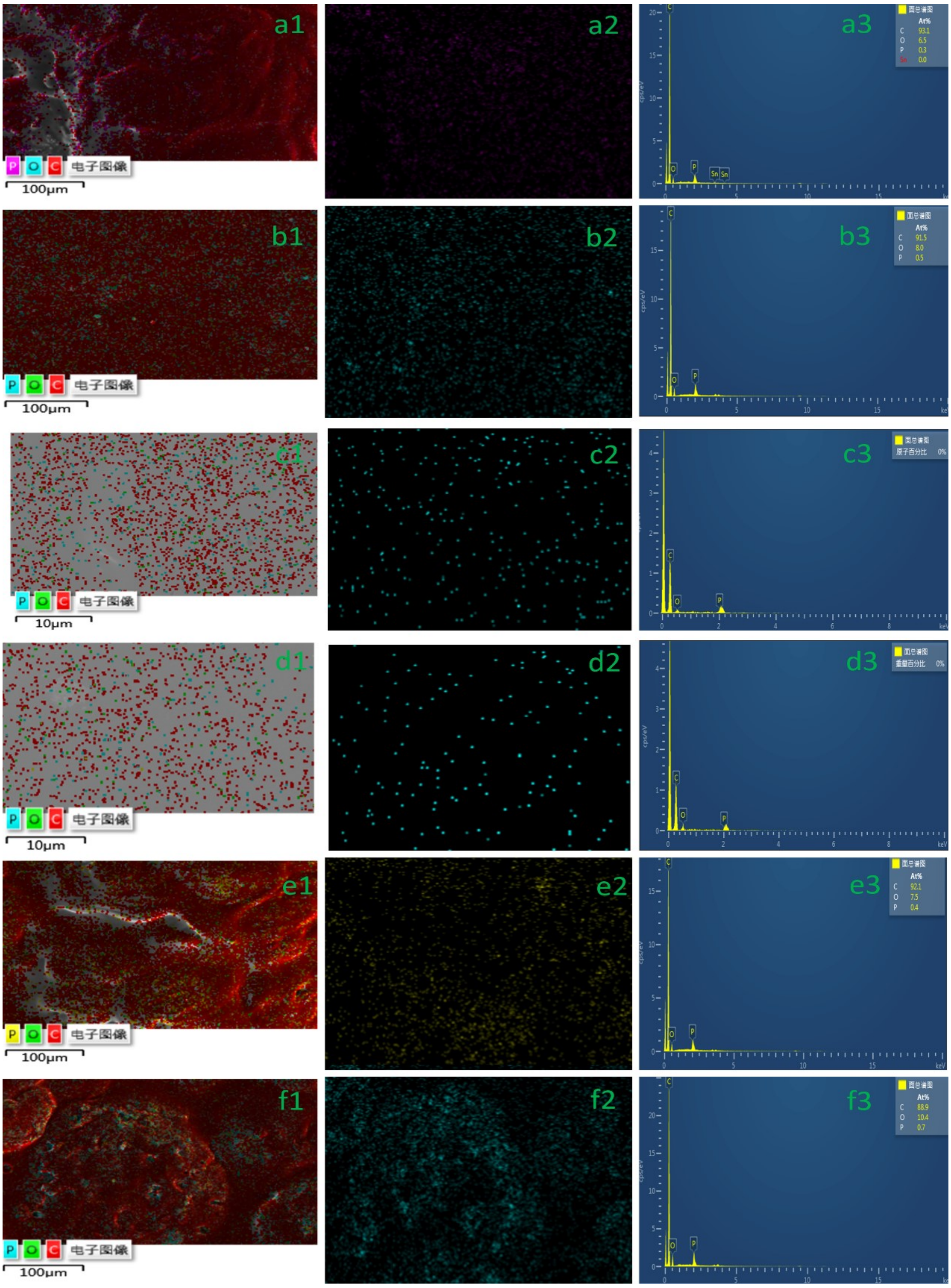

Fig. S11. The EDS results of carbon residues after cone calorimetry test. The EDS, phosphorus spectrum, and element contents of PDLA/5%R(-) (a1-a3), PDLA/5%L(+) (b1-b3), PLLA/5%R(-) (c1-c3), PLLA/5%L(+) (d1-d3), PMLA/5%R(-) (e1-e3), and PMLA/5%L(+) (f1-f3) compounds

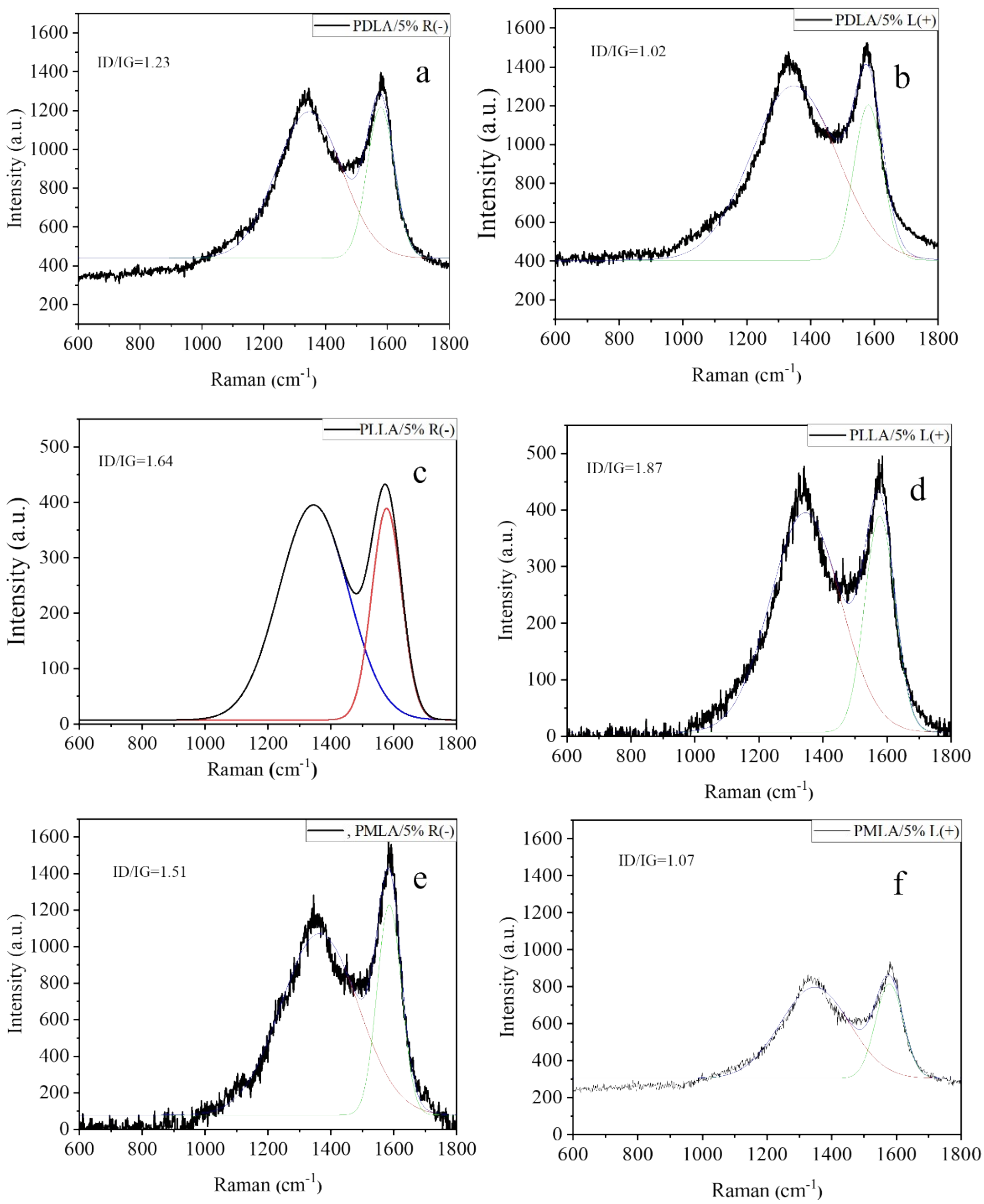

Fig. S12. The Raman spectra of carbon residues after cone calorimetry test. The Raman results of PDLA/5%R(-) (a), PDLA/5%L(+) (b), PLLA/5%R(-) (c), PLLA/5%L(+) (d), PMLA/5%R(-) (e), and PMLA/5%L(+) (f) compounds

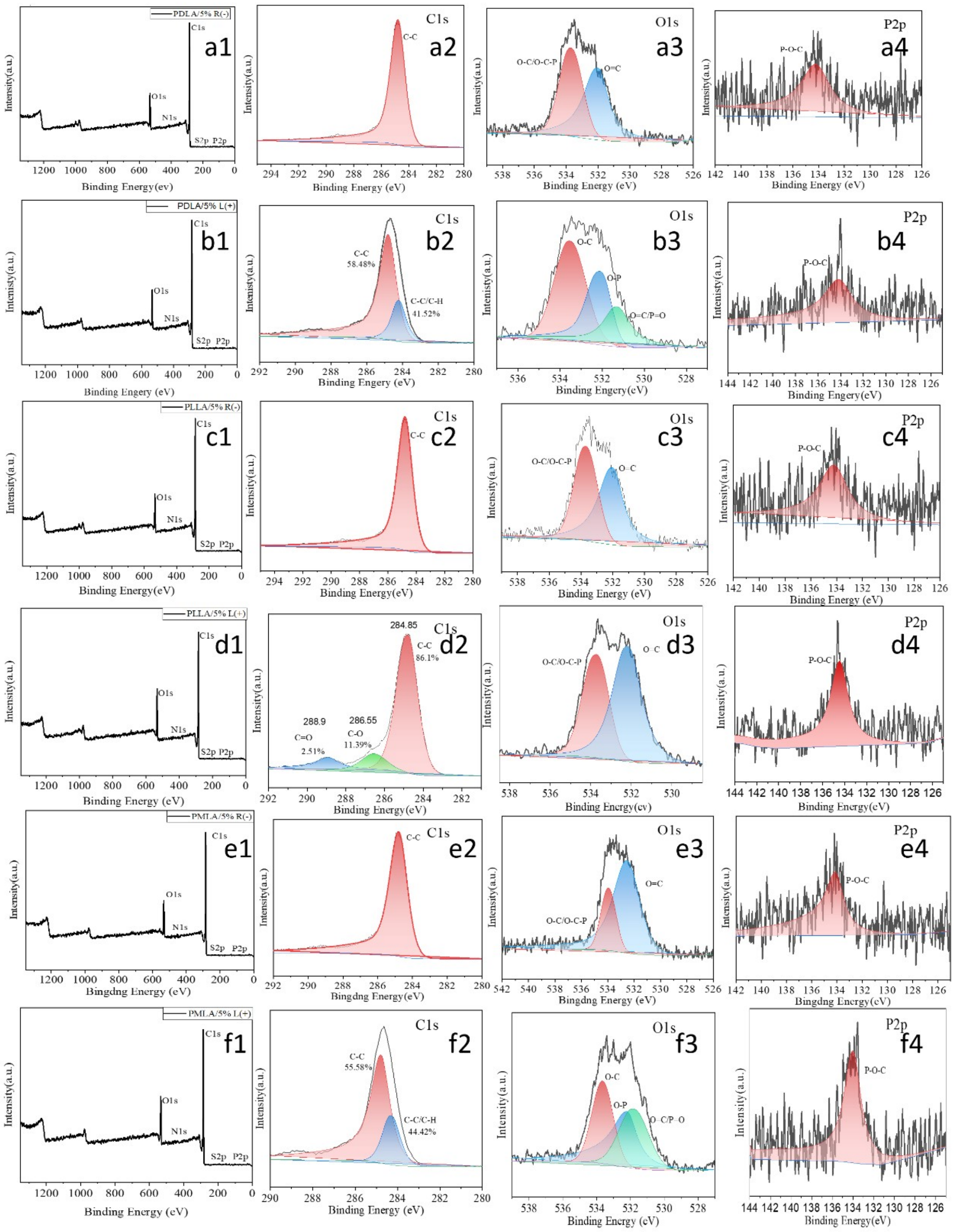

Fig. S13. The XPS results of carbon residues after cone calorimetry test. The XPS, C1s, O1s and P2p of PDLA/5%R(-) (a1-a4), PDLA/5%L(+) (b1-b4), PLLA/5%R(-) (c1-c4), PLLA/5%L(+) (d1-d4), PMLA/5%R(-) (e1-e4), and PMLA/5%L(+) (f1-f4) compounds

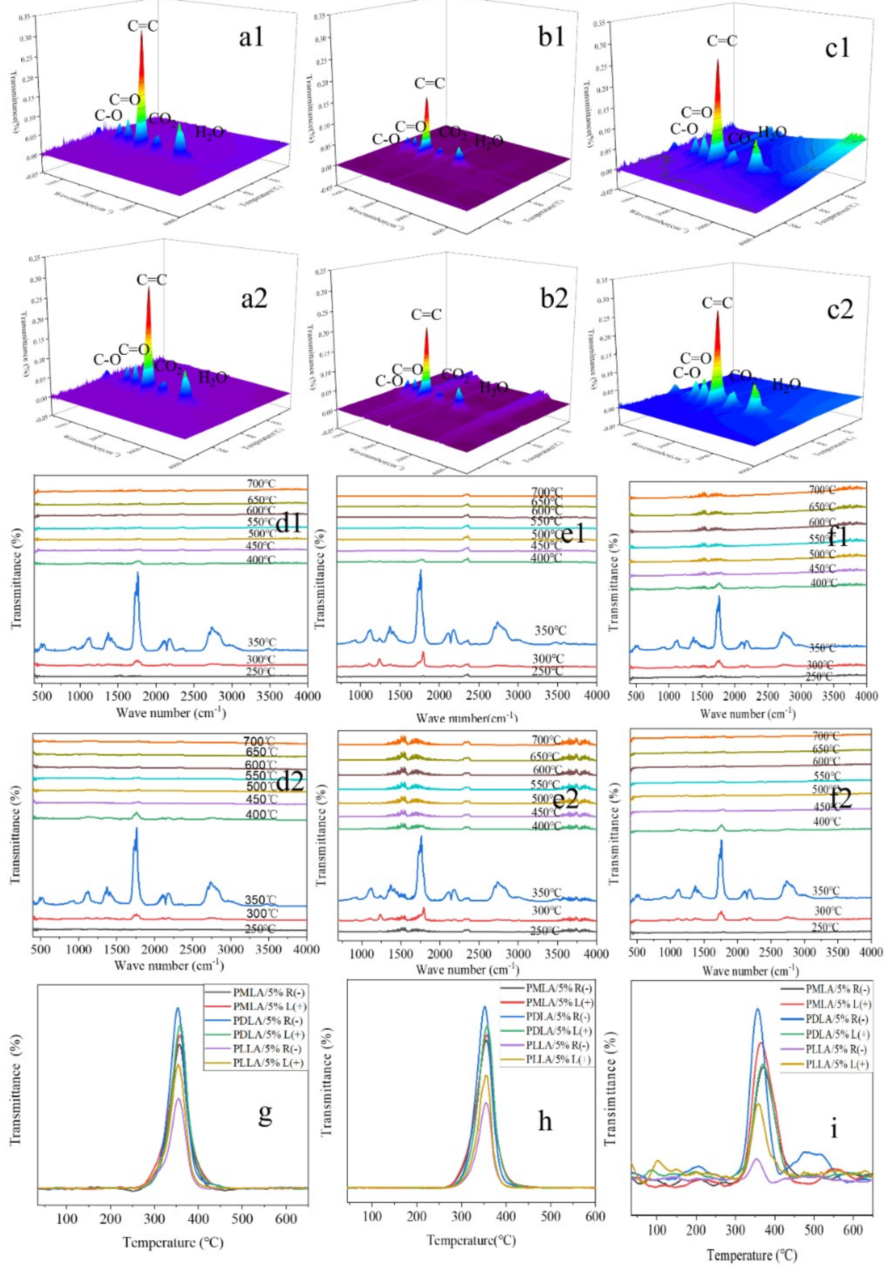

Fig. S14. Pyrolysis behavior in vapor phase. Three dimensions degradation of PDLA/5%R(-) (a1), PDLA/5%L(+) (a2), PLLA/5%R(-) (b1), PLLA/5%L(+) (b2), PMLA/5%R(-) (c1), and PMLA/5%L(+) (c2) compounds. TG-FTIR curves of PLA PDLA/5%R(-) (d1), PDLA/5%L(+) (d2), PLLA/5%R(-) (e1), PLLA/5%L(+) (e2), PMLA/5%R(-) (f1), and PMLA/5%L(+) (f2) compounds at different temperatures; the hydrocarbons (g), aldehydes (h), and carbonyl compounds (1) at different temperatures

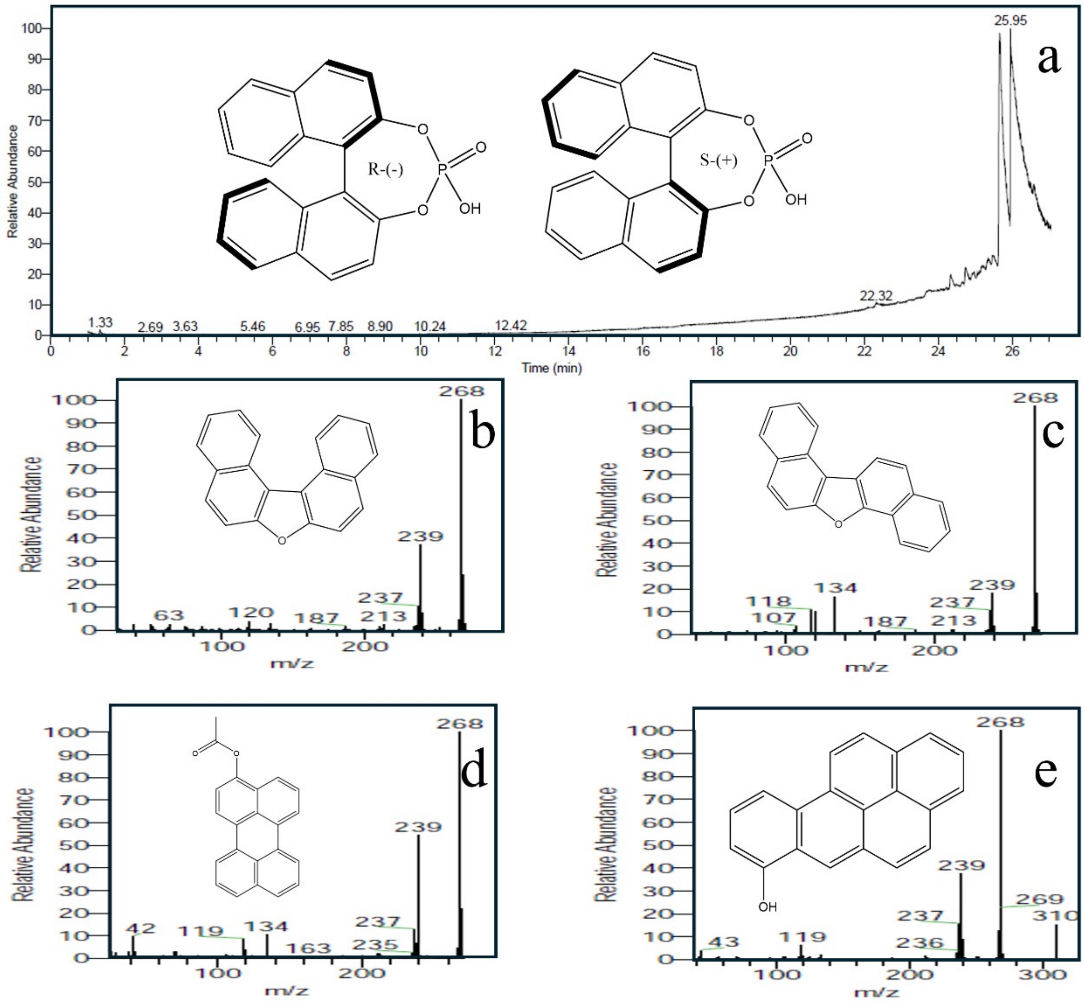

Fig. S15. The Py-GSMS results of (R)-(-)-1,1'-binaphthyl-2,2'-diyl hydrogen phosphate (R (-) flame retardant), and (S)-(+)-1,1'-binaphthyl-2,2'-diyl hydrogen phosphate (L (+) flame retardant), the keep time of R (-) and L (+) flame retardants (a), the main mass spectrometry of R (-) and L (+) flame retardants (b-e)

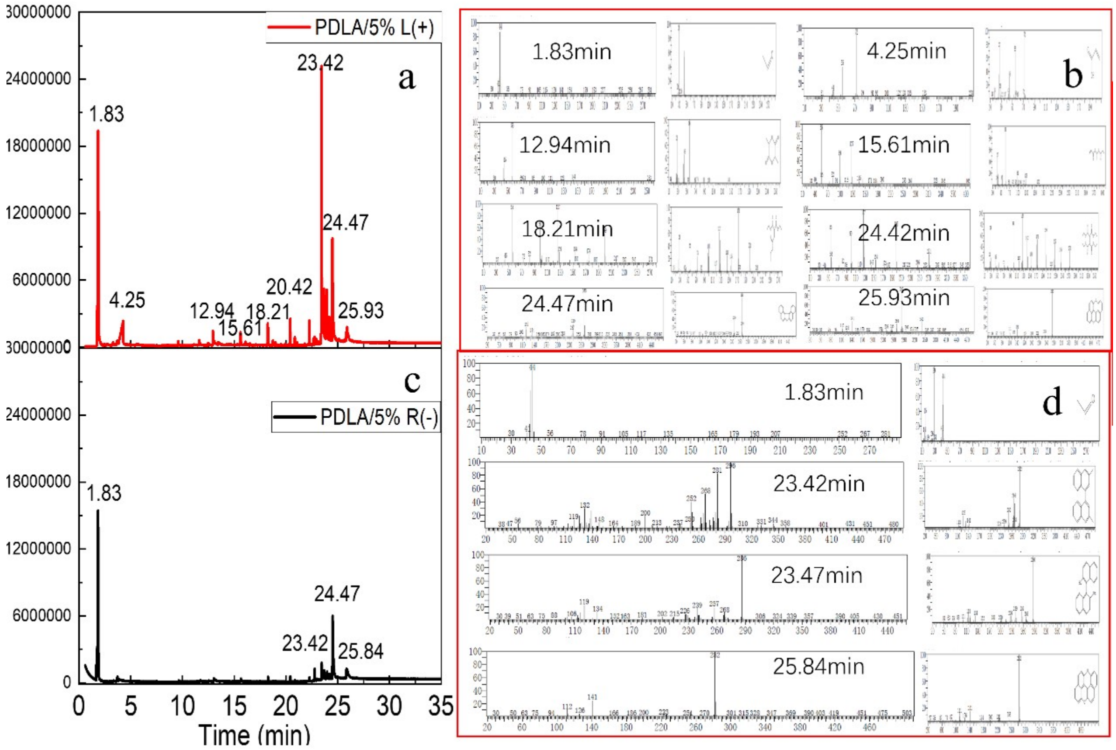

Fig. S16. The Py-GSMS results of PDLA/5%R(-) and PDLA/5%L(+) compounds. The keep time of PDLA/5%R(-) (c) and PDLA/5%L(+) compounds (a), the main mass spectrometry of PDLA/5%R(-) (d) and PDLA/5%L(+) compounds (b)

Table S1. Formula of functional PLA composites

Samples	Components (wt%)				FR loading (wt%)	P Contents （wt%）
	PDLA	PLLA	R	S		
PDLA	100	0	0	0	0	0
PLLA	0	100	0	0	0	0
PMLA	50	50	0	0	0	0
PDLA/1%R(-)	99	0	1	0	1	8.9×10^{-4}
PDLA/1%L(+)	99	0	0	1	1	8.9×10^{-4}
PDLA/5%R(-)	95	0	5	0	5	4.4×10^{-3}
PDLA/5%L(+)	95	0	0	5	5	4.4×10^{-3}
PLLA/1%R(-)	0	99	1	0	1	8.9×10^{-4}
PLLA/1%L(+)	0	99	0	1	1	8.9×10^{-4}
PLLA/5%R(-)	0	95	5	0	5	4.4×10^{-3}
PLLA/5%L(+)	0	95	0	5	5	4.4×10^{-3}
PMLA/1%R(-)	49.5	49.5	1	0	1	8.9×10^{-4}
PMLA/1%L(+)	49.5	49.5	0	1	1	8.9×10^{-4}
PMLA/5%R(-)	47.5	47.5	5	0	5	4.4×10^{-3}
PMLA/5%L(+)	47.5	47.5	0	5	5	4.4×10^{-3}

Table S2. The results of functional PLA composites in UL-94 and LOI tests

Samples	FR loading (wt%)	P Contents（wt%）	UL-94			LOI (%)
			$\bar{t}_1/\bar{t}_2$(s)	Ignition	Rating	
PDLA	0	0	＞30s/-	Y	NO*	19.5±0.0
PLLA	0	0	＞30s/-	Y	NO*	19.5±0.0
PMLA	0	0	＞30s/-	Y	NO*	19.5±0.1
PDLA/1%R(-)	1	8.9×10^{-4}	1.41s/1.23s	N	V-0	28.0±0.1
PDLA/1%L(+)	1	8.9×10^{-4}	1.21s/1.14s	N	V-0	28.5±0.2
PDLA/5%R(-)	5	4.4×10^{-3}	0.89s/0.72s	N	V-0	34.0±0.1
PDLA/5%L(+)	5	4.4×10^{-3}	0.81s/0.69s	N	V-0	34.5±0.2
PLLA/1%R(-)	1	8.9×10^{-4}	1.23s/1.20s	N	V-0	29.4±0.1
PLLA/1%L(+)	1	8.9×10^{-4}	1.53s/1.42s	N	V-0	27.5±0.1
PLLA/5%R(-)	5	4.4×10^{-3}	0.54s/0.62s	N	V-0	40.8±0.2
PLLA/5%L(+)	5	4.4×10^{-3}	1.01s/1.13s	N	V-0	30.9±0.1
PMLA/1%R(-)	1	8.9×10^{-4}	1.15s/1.02s	N	V-0	30.5±0.1
PMLA/1%L(+)	1	8.9×10^{-4}	1.02s/0.92s	N	V-0	32.0±0.2
PMLA/5%R(-)	5	4.4×10^{-3}	0.94s/1.01s	N	V-0	34.5±0.2
PMLA/5%L(+)	5	4.4×10^{-3}	0.83s/0.92s	N	V-0	36.0±0.1

* NO: no rating in UL-94 test

Table S3. The cone calorimeter results of functional PLA composites

Samples	HRR (kW/m^2)	THR ($MJ//m^2$)	SPR (m^2/s)	TSP (m^2)	COP (g/s)	CO_2P (g/s)
PDLA/5%R(-)	370	63.7	0.039	4.71	0.003	0.30
PDLA/5%L(+)	370	65.2	0.046	4.65	0.004	0.28
PLLA/5%R(-)	386	63.9	0.038	4.40	0.004	0.30
PLLA/5%L(+)	383	63.3	0.042	4.91	0.004	0.31
PMLA/5%R(-)	405	64.2	0.047	4.72	0.005	0.37
PMLA/5%L(+)	396	64.0	0.031	4.83	0.003	0.36

Table S4. The non-isothermal crystallization results of functional PLA composites

Samples	T_g (℃)	T_{cc} (℃)	T_m (℃)	ΔH_{cc} (J/g)	X_c (%)
PDLA	63.6	106.9	171.2	35.53	1.4
PLLA	63.8	107.3	170.3	36.64	1.5
PMLA	62.5	110.7	158.9/166.5	34.26	0.8
PDLA/1%R(-)	61.2	107.1	163.2	33.39	36.03
PDLA/1%L(+)	59.7	95.5	166.1	39.68	42.82
PDLA/5%R(-)	62.6	101.2	165.0	34.1	38.24
PDLA/5%L(+)	59.4	94.0	164.4	40.13	45.13
PLLA/1%R(-)	59.5	99.6	167.6	39.58	37.56
PLLA/1%L(+)	59.4	100.5	167.1	37.78	35.39
PLLA/5%R(-)	58.6	95.6	162.6/167.6	39.08	43.95
PLLA/5%L(+)	58.5	98.8	165.6	37.59	42.27
PMLA/1%R(-)	60.5	111.9	160/167	36.86	4.20
PMLA/1%L(+)	58.1	101.0	152.4/161.7	36.1	7.36
PMLA/5%R(-)	57.1	103.7	153/161.1	39.98	7.89
PMLA/5%L(+)	53.6	103.0	143.2/153.2	31.68	9.12

Table S5. The isothermal crystallization results of functional PDLA composites

Samples	T (°C)	n	lnk	k	$t_{1/2}$
PDLA/1%R(-)	100°C	2.56	-0.80717	4.5×10^{-1}	1.27
	105°C	1.75	0.19211	1.21	0.79
	110°C	1.63	0.48013	1.62	0.67
	115°C	2.63	1.43917	4.22	0.53
PDLA/1%L(+)	100°C	2.91	-0.13051	8.8×10^{-1}	0.97
	105°C	1.91	-0.081	9.2×10^{-1}	0.90
	110°C	1.71	-0.15151	8.6×10^{-1}	0.95
	115°C	2.49	0.70545	2.02	0.66
PDLA/5%R(-)	100°C	3.89	1.74876	5.74	0.56
	105°C	1.98	1.25065	3.49	0.47
	110°C	2.72	1.44851	4.26	0.53
	115°C	3.72	1.64569	5.18	0.56
PDLA/5%L(+)	100°C	2.39	2.27944	9.77	0.34
	105°C	2.11	1.08136	2.95	0.53
	110°C	2.10	0.92691	2.53	0.56
	115°C	3.39	1.78669	5.97	0.52

Table S6. The isothermal crystallization results of functional PLLA composites

Samples	T (°C)	n	lnk	k	$t_{1/2}$
PLLA	100	2.32	-2.47	8.64×10^{-2}	2.48
	105	2.34	-2.45	8.60×10^{-2}	2.44
	110	2.26	-1.14	3.20×10^{-1}	1.41
	115	2.36	-2.41	9.00×10^{-2}	2.38
PLLA/1%R(-)	100	2.20	-1.88624	1.52×10^{-1}	2.35
	105	2.25	-2.10087	1.22×10^{-1}	1.05
	110	2.33	-2.34343	9.56×10^{-2}	2.7
	115	2.09	-1.9591	1.41×10^{-1}	2.6
PLLA/1%L(+)	100	2.15	-1.68347	1.86×10^{-1}	2.2
	105	2.27	-2.2667	1.04×10^{-1}	1.1
	110	1.99	-1.68758	1.85×10^{-1}	2.45
	115	2.10	-1.63426	1.95×10^{-1}	2.2
PLLA/5%R(-)	100	2.06	-2.17288	1.13×10^{-1}	2.9
	105	1.85	-1.93064	1.45×10^{-1}	2.8
	110	2.16	-1.58073	2.06×10^{-1}	2.1
	115	2.05	-1.04996	3.49×10^{-1}	1.6
PLLA/5%L(+)	100	2.79	0.7024	2.06	0.85
	105	2.75	0.18935	1.21	1.0
	110	1.60	0.34358	1.41	0.9
	115	2.54	-0.65866	5.16×10^{-1}	1.3

Table S7. Related thermal stability data for functional PLA composites under N_2.

Samples	$T_{-5\%}$ (℃)	T_{max} (℃)	R_{max} (%/K)	Residual (%)		
				500℃	600℃	700℃
PDLA	333	369	3.14	0.13	0.05	0.03
PLLA	332	369	3.15	0.12	0.04	0.02
PMLA	336	366	3.37	1.21	0.83	0.75
PDLA/5%R(-)	300	350	2.32	1.41	1.22	1.03
PDLA/5%L(+)	296	345	2.13	1.55	1.39	1.24
PLLA/5%R(-)	302	351	2.12	2.00	1.71	1.69
PLLA/5%L(+)	302	352	2.21	1.78	1.54	1.53
PMLA/5%R(-)	296	347	2.51	2.07	1.96	1.82
PMLA/5%L(+)	279	347	2.25	1.95	1.77	1.73